Inorganic Chemistry

Article

pubs.acs.org/IC

Pressure Induced Crossover between a Ferromagnetic and a Canted Antiferromagnetic State for [Bis(pentamethylcyclopentadienyl)-iron(III)][Tetracyanoethenide], [$FeCp_2^*$][TCNE]

Jack G. DaSilva,[†] Rodolphe Clérac,[‡,§] and Joel S. Miller[†,*]

[†]Department of Chemistry, University of Utah, 315 S 1400 East, Salt Lake City, Utah 84112-0850, United States

[‡]CNRS, CRPP, UPR 8641, F-33600 Pessac, France

[§]Univ. Bordeaux, CRPP, UPR 8641, F-33600 Pessac, France

Supporting Information

ABSTRACT: The reversible hydrostatic pressure dependent DC magnetic behavior of the ferromagnetically ordered electron transfer salt $[Fe^{III}Cp_2^*]^{\bullet+}[TCNE]^{\bullet-}$ (Cp^* = pentamethylcyclopentadienide; TCNE = tetracyanoethylene) was studied up to 12.2 kbar. A significant departure from the ambient pressure ferromagnetic behavior was observed under pressure. The temperature dependent magnetization data were typical of a ferromagnet at ambient pressure but exhibited an extreme reduction with increasing applied pressure, while metamagnetic-like behavior was evident in the field dependent magnetization data at 4.2 kbar and above. Hence, the decrease of the intermolecular separations due to increasing pressure enhances the nearest neighbor couplings, leading to an increase in magnetic ordering temperature, T_c. Furthermore, the presence of a metamagnetic-like behavior suggests an increase of the antiferromagnetic contribution to the interchain interactions. The low field magnetization data indicate that spin canting is induced by pressure, leading to a canted antiferromagnetic phase with a much lower magnetization than the low-pressure ferromagnetic state. This unprecedented magnetic behavior is consistent with the field, temperature, and pressure dependences of the magnetization below 20 K.

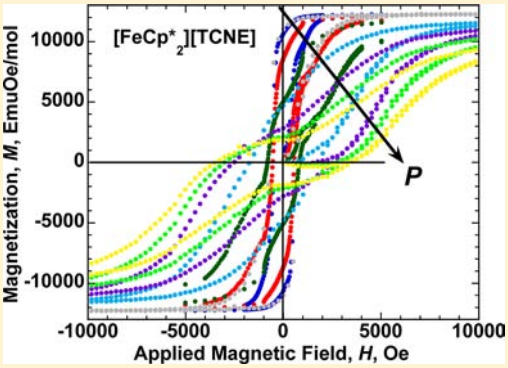

INTRODUCTION

Organic-based magnets[1] were first realized through the synthesis and study of [bis(pentamethylcyclopentadienyl)iron-(III)]$^+$[tetracyanoethenide]$^-$, $[Fe^{III}Cp_2^*]^{\bullet+}[TCNE]^{\bullet-}$, **1**, which magnetically orders below its ordering or critical temperature, T_c, of 4.8 K.[2−5] Ordering as a ferromagnet was ascertained from the saturation magnetization[4] and magnetic structure elucidated from neutron diffraction studies.[6] The discovery of ferromagnetic ordering in an organic-based magnet (OBM) has been of significant importance to theoretical solid-state physics and shows potential for accessing multifunctional materials.[7−10] $[FeCp_2^*]^{\bullet+}[TCNE]^{-\bullet}$ is an electron transfer salt possessing parallel linear chains of alternating S = 1/2$[FeCp_2^*]^{\bullet+}$ cations and S = 1/2$[TCNE]^{\bullet-}$ anions, with[11] and without solvent.[12,13] Several $[M^{III}Cp_2^*]^+[A]^{\bullet-}$ analogs have been synthesized through the variation of the paramagnetic metal center (M = Fe, Mn, Cr) and/or the cyanocarbon electron acceptor [A = TCNE, 7,7,8,8-tetracyano-*p*-quinodimethane (TCNQ), hexacyanobutadiene (HCBD), 2,3-dichloro-5,6-dicyanobenzoquinone (DDQ), and 2,3-dicyano-1,4-naphthoquinonide (DCNQ)].[5] This family of electron transfer salts has very similar structural motifs, which give rise to metamagnetic, ferromagnetic, and paramagnetic properties. For example, [$FeCp_2^*$][TCNQ] has been isolated as three polymorphs, each having a different magnetic ground state, namely, one each with an antiferromagnetic, ferromagnetic, and paramagnetic ground state.[5]

This suggests that the magnetic properties of this type of magnet are sensitive to the small variations in the nearest neighbor couplings arising from small structural differences within the family and perhaps the unique spin density of the various ligands, as computationally noted for $[FeCp_2^*]^{\bullet+}[TCNE]^{\bullet-}$.[11] The 10 pairwise nearest neighbor interactions identified for the 12 K structure of $[FeCp_2^*]^+[TCNE]^-$ were characterized by strong intrachain ferromagnetic coupling and weak (2 orders of magnitude smaller) interchain ferro- and antiferromagnetic couplings and proposed dipolar interactions. Thus, although the inter- and intrachain interactions are necessary for the existence of the 3-D magnetic order, the paramagnetic behavior above T_c is appropriately described by a 1-D spin model.[4] The presence of isolated ions in this family of compounds, i.e., their 0-D structural nature, presumably allows hydrostatic pressure to affect the magnetic interactions in all of the directions of the crystal lattice.

The previous hydrostatical pressure-dependent magnetic study of $[FeCp_2^*]^{\bullet+}[TCNE]^{\bullet-}$ based on AC susceptibility

Received: August 27, 2013
Published: September 23, 2013

   dx.doi.org/10.1021/ic4021959 | *Inorg. Chem.* 2013, 52, 11677−11683

Table 1. Summary of the 2 K Ambient and Pressure Dependent Magnetic Behavior of Polycrystalline $[FeCp_2^*][TCNE]$ (1), $[FeCp_2^*][C_4(CN)_6]$ (2), and the Ferromagnetic (FO) and Metamagnetic (MM) Polymorphs of $[FeCp_2^*][TCNQ]$

	P, kbar	method	T_c, K	rate,[a] K/kbar	ϕ[30]	T_b, K	rate,[a] K/kbar	H_{cr}, Oe	M(5 T), emu Oe/mol	M_r, emu Oe/mol
1	ambient	$M_r(T)$	4.8[4]			5.15		1000[e,4]	16 300[e,4]	15 600[e,4]
1	ambient	$M_r(T)$	5.11					540	12 800	10 500
1	12.2	$M_r(T)$	7.48	0.20		7.80	0.22	3450	11 000	10
1	ambient	ND[a]	4.74[27]							
1	ambient	C_p[b]	4.82[28]							
1	ambient	AC	4.95[c,12]		0.008					
1	ambient	AC	5.1[d,14]							
1	13.75	AC	7.85[14]	0.22[14]						
FO	ambient	AC	3.1[31]		0[31]				16 740[31]	
FO	ambient	$M_r(T)$	2.95[15]			2.92[15]			12 900[15]	
FO	10.3	$M_r(T)$	5.01[15]	0.21[15]		5.46[15]	0.25[15]	550[15]	11 000[15]	8880[15]
MM	ambient	AC	2.5[31]		0[31]					
MM	ambient	d(χT)/dT	2.10[15]						15 900[31]	
MM	2.9	d(χT)/dT	2.90[15]	0.28[15]					14 600[f,15]	
2	ambient	AC	2.93[16]		0.094[16]					
2	3.1	d(χT)/dT	2.46[16]					65[16]	50 400[16]	35[16]
2	11.4	d(χT)/dT	4.80[16]	0.28[16]				795[16]	13 100[16]	20[16]

[a]Neutron diffraction. [b]Heat capacity. [c]T_f (10 Hz). [d]T_f (16 Hz). [e]Aligned single crystal. [f]9.2 kbar.

data revealed low- and high-pressure regions of magnetic behavior, characterized by different rates of increase of the T_c. Above 5.30 kbar a new, higher-temperature magnetic AC peak was observed at a temperature denoted as T_1. Upon release of the applied pressure, the field dependent magnetization, $M(H)$, revealed complex hysteretic behavior, explained as an irreversible pressure-induced phase transition with incomplete conversion.[14] This effect was reinvestigated in order to clarify the origin of pressure-induced formation of the metamagnetic-like behavior, as well as understand the increase in T_c with increasing pressure.

In addition, the pressure dependence for $[FeCp_2^*][TCNE]$ is compared with that recently reported for the similarly structured ferromagnetic (**FO**) and metamagnetic (**MM**) polymorphs of $[FeCp_2^*][TCNQ]$,[15] $[FeCp_2^*][C_4(CN)_6]$,[16] $[FeCp_2^*][DDQ]$,[16] and $[FeCp_2^*][DCNQ]$,[17] as well as other TCNE-based magnets including 1-D [MnTRPP][TCNE] [H_2TRPP = *meso*-tetrakis(4-R-substitutedphenyl)porphyrin; R = $OC_{10}H_{21}$, $OC_{14}H_{29}$, F],[18] 2-D $Mn^{II}(TCNE)I(OH_2)$, and 3-D $Mn^{II}(TCNE)_{3/2}(I_3)_{1/2}\cdot z$THF[19] and $Mn^{II}(TCNE)[C_4(CN)_8]_{1/2}\cdot z CH_2Cl_2$.[20] In addition to these materials, pressure also has been used to study other organic-based magnets,[21] and both the enhancement of T_c, e.g., β-4′-cyanotetrafluorophenyldithiadiazolyl][22] and benzo(1,2-d′:bis-[1,3,2]dithiazole) tetrachlorogallate,[23] and the reduction of T_c, e.g., 4-nitrophenylnitronyl nitroxide[24] and $[TDAE]^+[C_{60}]^-$ [TDAE = tetrakis(dimethylamino)ethane],[25] have been observed.

EXPERIMENTAL SECTION

$[FeCp_2^*]^+[TCNE]^-$ was prepared via the literature method.[3] IR and AC susceptibility measurements were used to confirm the purity of the sample. IR spectra were measured from 400 to 4000 cm^{-1} on a Bruker Tensor 37 spectrometer ($\pm$1 cm^{-1}). A Quantum Design Physical Property Measurement System QD (PPMS 9T) was used to perform ambient pressure AC susceptibility magnetometry. Ground samples of **1** (3−15 mg) were loaded into gelatin capsules in a glovebox atmosphere and sealed with silicone grease prior to PPMS measurements. A Quantum Design Superconducting Quantum Interference Device (SQUID) Magnetic Property Measurement System (MPMS-5XL 5 T; sensitivity = 10^{-8} emu or 10^{-12} emu/Oe at 1 T) was used to perform DC pressure dependent measurements, as previously described.[26] Samples of **1** (~1 mg) were loaded into a Teflon cell; the remaining volume of the Teflon cell was filled with decalin (the hydrostatic pressure media) and capped with Teflon plugs. The loaded Teflon sample cell was placed in a beryllium−copper hydrostatic pressure cell fabricated at the University of Utah based on the Kyowa Seisakusho design with zirconia pistons and rubber o-rings. Pressure was applied to the assemblage by using a Kyowa Seisakusho CR-PSC-KY05-1 apparatus with a WG-KY03-3 pressure sensor. The Aikoh Engineering Model-0218B digital sensor readout is an approximate method for determining pressure, and a superconductor with a known pressure dependent transition temperature has been used in previous magnetic studies to calibrate the pressure. Since T_c between 2 and 8 K is expected for **1**,[14] no convenient superconducting pressure calibrant was suitable. As reported for $[FeCp_2^*][TCNQ]$,[15] calibration was achieved from a least-squares linear regression fit $P = 0.025x - 0.7$, where x is the readout from the digital sensor from previous pressure data. The error associated with this correlated fit was assumed to be the standard deviation of the slope and intercept of the linear regression fit propagated through the pressure determination and is 0.048 kbar (χ^2 = 0.953).

The T_c was determined from the extrapolation of the most linear portion of the remnant magnetization, $M_r(T)$, to zero magnetization. Isothermal field dependent measurements, $M(H)$, were performed at 2 K, with a field sweep rate of 40, 267, and 5000 Oe/min in the ranges of $\pm$1, |1 − 5|, and |5 − 50| kOe, respectively, for $\leq$4.2 kbar, and 469 and 7000 Oe/min in the range $\pm$15 and |15 − 50| kOe, respectively, above 4.2 kbar. The coercive field, H_{cr}, was determined from the extrapolation of the field intercept at zero magnetization upon reduction of an applied field of $\pm$50 kOe, and the M_r was determined from the extrapolation of the magnetization intercept at zero applied field upon reducing the applied field from 50 kOe.

RESULTS AND DISCUSSION

Prior to the pressure dependence study of the magnetic properties of $[FeCp_2^*][TCNE]$, the ambient pressure magnetic properties were determined and compared to that previously reported to confirm the sample purity. Randomly orientated polycrystalline samples were prepared, as this was needed for the hydrostatic pressure studies. The T_c was determined to be 5.11 $\pm$ 0.03 K from 5-Oe DC remnant magnetization, $M_r(T)$, measurements and 5.00 $\pm$ 0.01 K determined as the peak of

dx.doi.org/10.1021/ic4021959 | Inorg. Chem. 2013, 52, 11677−11683

$\chi'(T)$ at 10 Hz at ambient pressure. This is in agreement with 4.8 K from $M_r(T)$[4] and neutron diffraction,[6] 4.74[27] and 4.82 K,[28] from adiabatic calorimetry utilizing the drift method.[29] The 2 K coercive field, H_{cr}, was 540 ± 10 of Oe. The saturation magnetization, M_s, was 12 800 emu Oe/mol, and the remnant magnetization, M_r, (magnetization at H = 0 in the hysteresis M vs H cycle from positive DC fields) was 10 500 emu Oe/mol. The H_{cr}, M_r, and M_s were expectedly reduced from 1000 Oe, 15 500 emu Oe/mol, and 16 300 emu Oe/mol, respectively[4] (Table 1), that were obtained for large aligned single crystals, that are very anisotropic,[3,4] but not for the randomly orientated polycrystalline samples that were studied herein.

The DC magnetization of [$FeCp_2$*][TCNE] as a function of temperature, field, and pressure was investigated to complement the previous pressure dependence of the AC susceptibility.[14] Overall, there is general agreement with the previous DC and AC susceptibility measurements as $T_c(P)$ increases with increasing pressure.

The pressure dependences of the 5-Oe remnant magnetization, $M_r(T)$, show that the onset temperature (T_c) at 5.11 K at ambient pressure increases with applied pressure to 7.48 K at 12.2 ± 0.83 kbar, Figures 1 and 2. This T_c increase corresponds

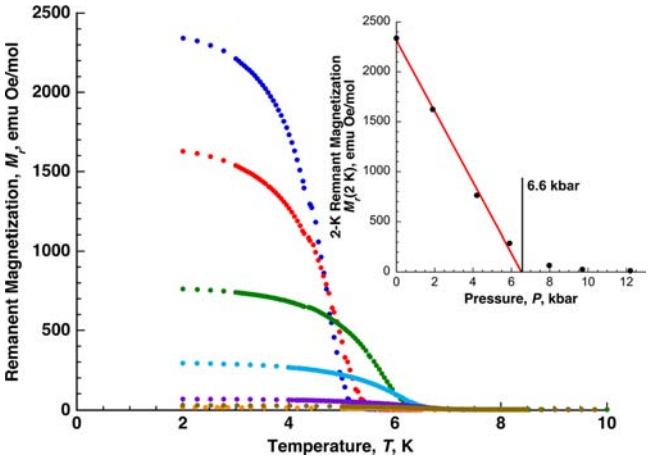

Figure 1. Pressure dependence of 5-Oe $M_r(T)$ of [$FeCp_2$*][TCNE] at 0.001 (blue), 1.9 (red), 4.2 (green), 5.9 (cyan), 8.0 (purple), 9.7 (brown), and 12.2 (orange) kbar. Inset: Pressure dependence of the 5-Oe remnant magnetization at 2 K. The solid red line is the linear fit of the pressure decrease of the 5-Oe remnant magnetization.

to a 46.4% rise at an average rate of 0.21 ± 0.02 K/kbar, Figure 2. This is in accord with the previously reported value from AC data, ~0.22 K/kbar.[14] Nevertheless, a crossover around 6.6 ± 1.5 kbar between two linear regimes is clearly observed in Figure 2. T_c increases linearly with the applied pressure up to about 6.6 kbar with a rate of 0.25 ± 0.02 K/kbar and then with a rate of 0.15 ± 0.04 K/kbar above 6.6 kbar. Concomitantly, the 5-Oe remnant magnetization dramatically decreases by 2 orders of magnitude from 2345 emu Oe/mol at ambient pressure to ~10 emu Oe/mol at 12.2 kbar (Figure 1).

The 5-Oe remnant magnetization decreases almost linearly between ambient pressure and ~6.6 kbar (Figure 1). Above this pressure, which also corresponds to the crossover pressure observed for the rate of change for the critical temperature with respect to pressure, $\Delta T_c/\Delta P$ (Figure 2), the remnant magnetization is very small (<100 emu Oe/mol), indicating the disappearance of the ferromagnetic ordered phase and appearance of an ordered magnetic phase with a nonzero, but

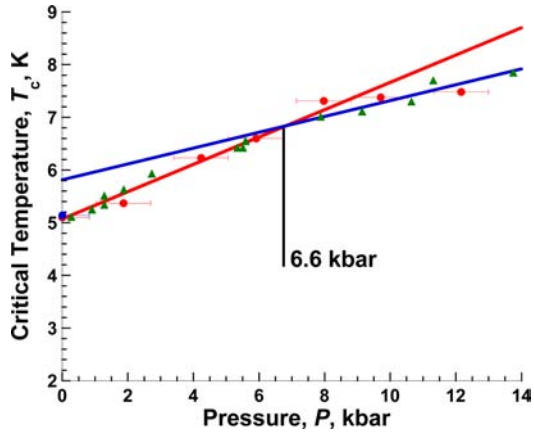

Figure 2. $T_c(P)$ (●) determined from the $M_r(T,P,5\ Oe)$ data shown in Figure 1 for [$FeCp_2$*][TCNE] (the T_c after released pressure is shown as a blue symbol). The temperature error bars are obscured by the data points. $T_c(P)$ (▲) previously reported from AC susceptibility data.[14] The solid red and blue lines are linear fits of all the DC and AC data below 5.9 K and above 5.6 K, as described in the text.

small spontaneous magnetization. This high-pressure magnetic phase is attributed to a canted antiferromagnetic (weak ferromagnet) ordered state[32] that is also consistent with the pressure dependence of the hysteretic data, $M(H)$, Figure 3.

The 2 K $M(H)$ data have a H_{cr}, M_r, and M_s of 540 Oe, 10 500 emu Oe/mol, and 12 800 emu Oe/mol, respectively at ambient pressure. With increasing applied pressure, the H_{cr} gradually increases up to ~4 kbar and then more steeply to 3520 Oe at 12.2 kbar, Figures 3 and 4. The change of regime in the H_{cr} increase coincides with the crossover observed around 6.6 ± 1.5 kbar for the $T_c(P)$, Figure 2, and $M_r(P)$, Figure 1. Concomitantly, the M_r and M_s values extracted from the 2 K $M(H)$ data also decrease upon pressure change with different variations, as illustrated in Figure 4.

The fact that the M_r decreases faster (from 10 500 emu Oe/mol at ambient pressure to 1840 emu Oe/mol at 12.2 kbar, a 82% reduction) than M_s (from 12 800 emu Oe/mol at ambient pressure to 10 994 emu Oe/mol at 12.2 kbar, only a 14% reduction) especially above 4 kbar implies canting of the two sublattices in the magnetically ordered phase. The canting angle is determined from $2\arccos[2M_r(P)/M_s(P)]$.[33] Note in contrast to ref 33, the angle of the two limiting cases for ferro- and antiferromagnetic phases has been defined at 0° and 180°, respectively.[34] The pressure variation of the canting angle is given in Figure 5. Below 5.9 kbar, the M_r/M_s ratio is larger than 0.5. Thus, the ordered magnetic phase is ferromagnetic, and the two sublattices are parallel (i.e., a 0° canting angle). At 5.9 kbar, the M_r value is reduced significantly in comparison to M_s, and only a canting of the two sublattices can explain this result. The canting angle at 5.9 kbar is ~74°, and it reaches 141° at 12.2 kbar with a quasi-saturation that suggests that the antiferromagnetic phase (i.e., an 180° canting angle) is not attained even at higher pressure in the absence of a high pressure structural transition.

These results are in accord with a decrease of the intermolecular separations induced by the applied pressure, which in turn enhances the nearest neighbor intra- and interchain couplings and thus increases T_c (Figure 2). Concomitantly, the 5-Oe remnant magnetization decreases, indicating that the magnetic moments cant to reduce the magnetization with increasing pressure and thus are not

dx.doi.org/10.1021/ic4021959 | Inorg. Chem. 2013, 52, 11677−11683

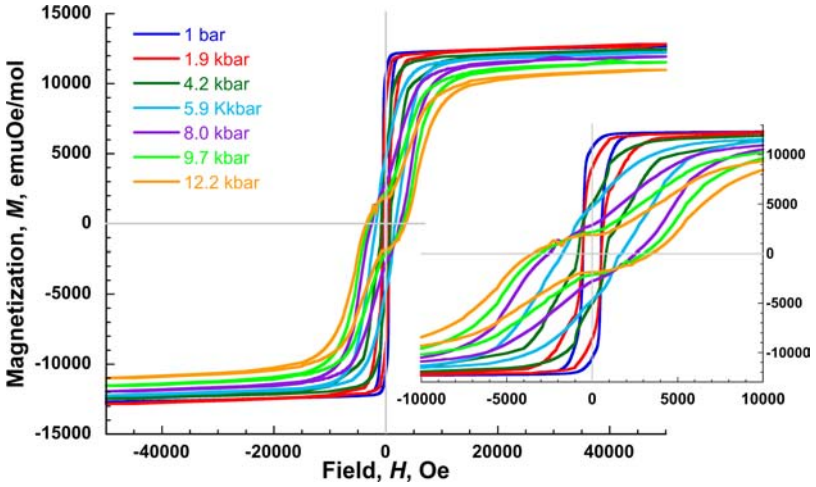

Figure 3. 2-K hysteretic $M(H,P)$ plots of $[FeCp_2^*]^+[TCNE]^-$ at 0.001 (blue), 1.9 (red), 4.2 (green), 5.9 (cyan), 8.0 (purple), 9.7 (neon green), and 12.2 (orange) kbar. Note that the data after pressure was released gave reproducible data.

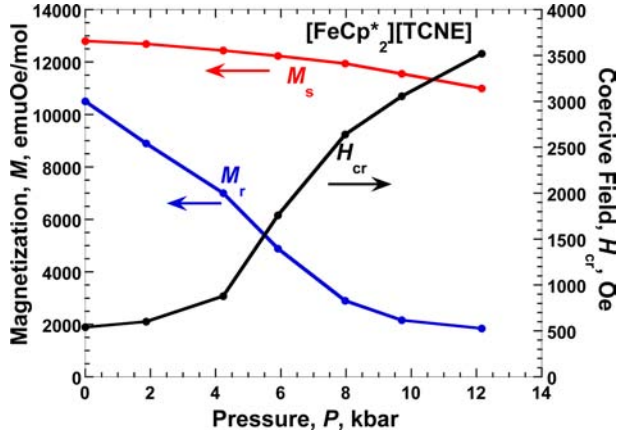

Figure 4. The 2 K coercive field, $H_{cr}(P)$ (black ●), magnetization at 5 T considered at saturation, $M_s(P)$ (red ●), and remnant magnetization (magnetization value at $H = 0$ in the hysteresis M vs H cycle from positive DC fields), $M_r(P)$ (blue ●) of $[FeCp_2^*][TCNE]$. The lines are guides for the eyes.

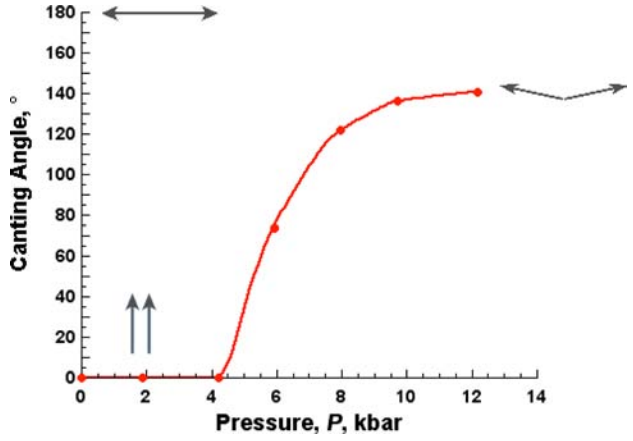

Figure 5. Pressure dependence of the canting angle between the two sublattices in $[FeCp_2^*][TCNE]$ at 2 K. This angle is calculated from the $M_s(P)$ and $M_r(P)$ values shown in Figure 4 for a canting antiferromagnetic phase: canting angle = $2\arccos[2M_r(P)/M_s(P)]$.[33] The lines are guides for the eyes.

anymore perfectly ferromagnetically aligned. Above 6.6 kbar, the remnant magnetization is very small, indicating a large canting angle between two antiferromagnetically coupled magnetic sublattices. As suggested by the previous AC susceptibility measurements above 5.30 kbar,[14] a crossover between 4 and 7 kbar from a ferromagnet to a canted antiferromagnet is clearly observed as the canting angle increases with applied pressure while the magnetization dramatically decreases. Additionally, the intrachain collinear ferromagnetic coupling between the $S = 1/2$ $[Fe^{III}Cp_2^*]^{\bullet+}$ and $S = 1/2$ $[TCNE]^{\bullet-}$ lattices[11] may also cant with increasing pressure, and also contribute to the canted antiferromagnetic behavior.

Note that the shape of the hysteresis loop is also qualitatively altered at 4.2 kbar. At higher pressures, the hysteresis loop resembles that of a canted antiferromagnet with a metamagnetic-like behavior, with a large coercive field and an *S*-shaped variation.[5,33] Unfortunately, due to the large magnetic hysteresis, it is not possible to separate (even on the first magnetization curve) the effects of the magnetic domain reorientation and the metamagnetic critical field that both lead to the *S*-shaped signatures in the same DC field region. It should be noted that *S*-shaped virgin curves are also suggestive of spin glass behavior in ferromagnetic materials,[35] and spin glass behavior has been observed for **1** from AC studies, for which the figure of merit, ϕ, is 0.008.[14,30]

The pressure-induced crossover between the ferro- and canted antiferromagnetic states was further investigated through the temperature dependences of the field-cooled magnetization, $M_{FC}(T)$, at different applied pressures (a representative behavior is shown at 500 Oe in Figure 6; the data at other DC fields are shown in the Supporting Information) and several applied fields (a representative behavior is shown at 6.5 kbar in Figure 7; the data at other pressures are shown in the Supporting Information). Below 4.2 kbar, the $M_{FC}(T, 500\ Oe)$ data are typical of a ferromagnetic state with a rapid increase of the magnetization at the transition temperature (Figure 2). Between 4.2 and 5.1 kbar, a shoulder appears for the $M_{FC}(T)$ data around 7.5 K, and a clear maximum is observed at higher pressures. This is the signature of the ordered canted antiferromagnetic phase (Figures 6). This behavior further confirms the crossover between a ferromagnetic state at low pressure and a canted antiferromagnetic state

dx.doi.org/10.1021/ic4021959 | Inorg. Chem. 2013, 52, 11677−11683

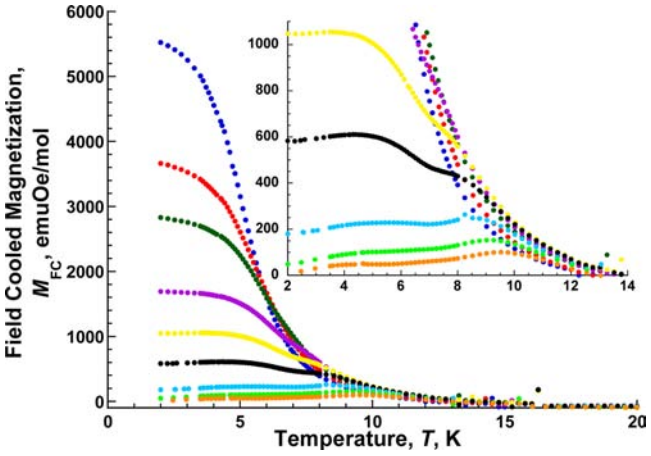

Figure 6. $M_{FC}(T,P,$ 500 Oe) at 0.4 (blue), 2.2 (red), 3.1 (green), 4.2 (purple), 5.1 (yellow), 6.5 (black), 8.0 (cyan), 9.9 (neon green), and 12.2 (orange) kbar. Inset displays a zoomed view about the 5.1 kbar and greater applied pressure measurements. These data are representative of the data obtained at other applied fields, see Figures S1−S11.

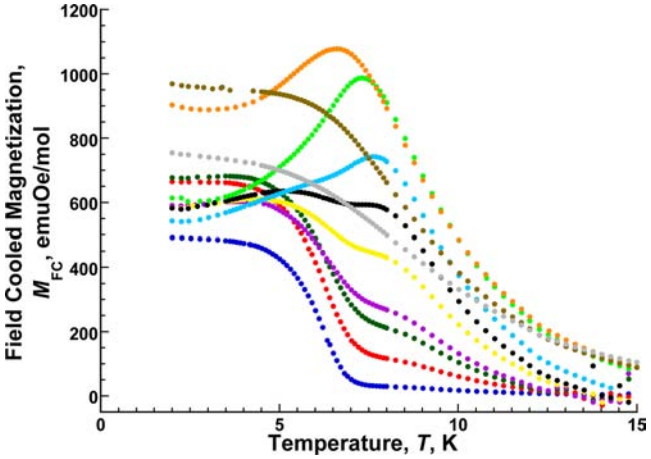

Figure 7. $M_{FC}(T,H,$6.5 kbar) at 20 (blue), 100 (red), 200 (green), 300 (purple), 500 (yellow), 700 (black), 1000 (cyan), 1500 (neon green), 2000 (orange), 3000 (dark green), and 5000 Oe (gray). These data are representative of the data obtained at other pressures, see Figures S12−S20.

stabilized above 4.2 kbar,[36] as is also suggested by previous AC measurements and the appearance of the aforementioned peak in the susceptibility data at T_1.[14]

In the canted antiferromagnetic phase at 6.5 kbar (Figures 7), the noncompensation of the two antiferromagnetically coupled sublattices is seen at ∼20 Oe with a rapid increase of the magnetization similar to the ferromagnetic phase (at 0.4 kbar), but with a much lower magnetization at 2 K (490 vs 4700 emu Oe/mol at 20 Oe). At higher DC fields, a shoulder around 8.5 K is first seen between 100 and 700 Oe before observing a clear maximum at 7.7 K at 1000 Oe. At and above 3000 Oe, the maximum in the magnetization disappears as is expected above the spin-flip field characteristic of metamagnetic behavior. These magnetization data clearly confirm the presence of a canted antiferromagnetic phase above 4.2 kbar with a metamagnetic-like behavior under a DC field.

The pressure dependent magnetic behavior of [$FeCp_2$*][TCNE] (**1**) is similar to that of structurally related [$FeCp_2$*][$C_4(CN)_6$] (**2**),[16] [$FeCp_2$*][DCNQ],[17] and the metamagnetic (**MM**) and ferromagnetic (**FO**) polymorphs of [$FeCp_2$*][TCNQ][15] as T_c increases with increasing pressure, but other aspects of the magnetic behaviors including the ground and higher pressure magnetic states differ. [$FeCp_2$*][$C_4(CN)_6$] differs from [$FeCp_2$*][TCNE] as it does not magnetically order with a spin-glass state at ambient pressure but, above 3.1 kbar, exhibits metamagnetic behavior with hysteresis indicative of a weak ferromagnet (canted antiferromagnet), and above 3.1 kbar its coercive field increases with increasing pressure, while the remnant magnetization decreases with increasing pressure, as observed for [$FeCp_2$*][TCNE].[16]

The ferromagnetic polymorph of [$FeCp_2$*][TCNQ] (**FO**) has a similar increase in $T_c(P)$ and decrease in the 50-kOe magnetization to [$FeCp_2$*][TCNE]. Likewise, the coercivity of both of these ferromagnets increases with increasing pressure; however, [$FeCp_2$*][TCNQ] does not exhibit a transition to a canted antiferromagnet below 10.3 kbar, and unlike [$FeCp_2$*][TCNE] its remnant magnetization increases with increasing pressure.[15] In contrast, the metamagnetic polymorph (**MM**) has an antiferromagnetic ground state whose $T_c(P)$ also increases with increasing pressure, as does metamagnetic critical field, $H_c(P)$. However, above 3.9 kbar, a transition to a paramagnetic state occurs.[15] [$FeCp_2$*][DCNQ], like the metamagnetic phase of [$FeCp_2$*][TCNQ], has its $T_c(P)$ and $H_c(P)$ increase with increasing pressure; however, a transition to a paramagnetic state was not reported.[17] Hence, albeit structurally quite similar, differing electron acceptors lead to different magnetic behaviors, Table 2, and theoretical insight and computational support are needed to identify the competing interactions and their magnitudes, which are modified under hydrostatic pressure.

Table 2. Summary of the Magnetic Behavior[a] at Ambient and High Pressure for [$FeCp_2$*][TCNE] (1), [$FeCp_2$*][$C_4(CN)_6$] (2), and the Ferromagnetic (FO) and Metamagnetic (MM) Polymorphs of [$FeCp_2$*][TCNQ]

	ground magnetic state, 1 atm	$P >$ ambient	transition pressure, kbar	ref
[$FeCp_2$*][TCNE]	FO	CW	∼6.6	this work
[$FeCp_2$*][$C_4(CN)_6$]	SG	AF/CW	∼3.1	16
[$FeCp_2$*][TCNQ], **MM**	AF/MM	P	∼2.9	15
[$FeCp_2$*][TCNQ], **FO**	FO	FO		15
[$FeCp_2$*][DDQ]	P	P		16
[$FeCp_2$*][DCNQ]	AF/MM	AF/MM		17

[a]FO = ferromagnet; AF = antiferromagnet; SG = spin glass; CW = weak ferromagnet (canted antiferromagnet); *P* = paramagnet; MM = metamagnet.

Furthermore, the pressure dependent behavior of [$FeCp_2$*][TCNE] is more complex than that observed for 1-D [MnTRPP][TCNE] [H_2TRPP = *meso*-tetrakis(4-R-substitutedphenyl)porphyrin; R = $OC_{10}H_{21}$, $OC_{14}H_{29}$, F], which undergoes a decrease in $T_c(P)$ with a small applied pressure, before reaching a minimum, and then $T_c(P)$ increases with additional increasing pressure, or 2-D,[18] layered $Mn^{II}(TCNE)I(OH_2)$ and 3-D structured

dx.doi.org/10.1021/ic4021959 | *Inorg. Chem.* 2013, 52, 11677−11683

$Mn^{II}(TCNE)_{3/2}(I_3)_{1/2}\cdot zTHF$[19] for which $T_c(P)$ increases with increasing pressure but does not have pressure dependent magnetic transition to a different magnetic state. The rate of increase of $T_c(P)$ for the $FeCp_2^*$-based magnets, 0.24 ± 0.04 K/kbar (Table 1), however, is substantially reduced from 6.6 to 7.1 K/kbar reported for $Mn^{II}(TCNE)I(OH_2)$ and $Mn^{II}(TCNE)_{3/2}(I_3)_{1/2}$.[19] In contrast, in addition to having a substantially larger $dT_c(P)/dT$, 3-D network structured $Mn^{II}(TCNE)[C_4(CN)_8]_{1/2}\cdot zCH_2Cl_2$[20] and $[Ru_2(O_2CMe)_4]_3[Cr(CN)_6]$[37] undergo different types of magnetic transitions.

CONCLUSION

The pressure dependent DC magnetic investigation of $[FeCp_2^*][TCNE]$ yielded an enhancement of the T_c from 5.11 K at ambient pressure to 7.48 K at 12.2 kbar in agreement with previous AC data under pressure.[14] A clear crossover between two linear regimes of T_c (with rates of 0.25 and 0.15 K/kbar below and above 6.6 ± 1.5 kbar, respectively) are observed around 6.6 kbar. Concomitantly, the 5-Oe remnant magnetization dramatically decreases by 2 orders of magnitude, indicating a partial compensation of the magnetic moment in the ordered phase. The detailed analysis of the 2 K $M(H)$ hysteresis curves as a function of the applied pressure confirmed the observed crossover that was unambiguously attributed to a change of magnetic ground state from an ordered ferromagnetic phase below 4.2 kbar (as previously reported[2−5,11]) to an ordered canted antiferromagnetic phase at 5.9 kbar and above. The canting angle that reaches 141° at 12.2 kbar was evaluated from the magnetization at saturation under 5 T and from the remnant magnetization determined on the $M(H)$ hysteresis loops at different applied pressures. With increasing pressure, the intermolecular separations decrease, increasing the nearest neighbor ferromagnetic and antiferromagnetic couplings,[11] that in turn increases the T_c, while these competing couplings lead to canting that is enhanced with increasing pressure. Thus, the magnetization dramatically decreases with applied pressure. Future structure determinations as a function of pressure and supporting theoretical and computational investigations enabling the prediction of the pressure dependence of the couplings should identify the origins of the unique magnetic behavior of $[FeCp_2^*][TCNE]$.

ASSOCIATED CONTENT

Supporting Information

$M_{FC}(T,P)$ as a function of applied field and $M_{FC}(T,H)$ as a function of applied pressure. This material is available free of charge via the Internet at http://pubs.acs.org

AUTHOR INFORMATION

Corresponding Author

*E-mail: jsmiller@chem.utah.edu.

Notes

The authors declare no competing financial interest.

ACKNOWLEDGMENTS

J.G.D. and J.S.M. appreciate Royce A. Davidson's assistance with diamagnetic corrections due to the excessive mass of the BeCu pressure apparatus, the helpful discussion with John C. Conboy, the continued support by the Department of Energy Division of Material Science (Grant Nos. DE-FG03-93ER45504) for the chemical synthesis and magnetization studies, as well as the Conseil Régional d'Aquitaine, the Université of Bordeaux, and the CNRS (R.C.) for theoretical insight. All authors contributed to the writing of the manuscript.

REFERENCES

(1) (a) Blundell, S. J.; Pratt, F. L. *J. Phys.: Condens. Matter* **2004**, *16*, R771. (b) Ovcharenko, V. I.; Sagdeev, R. Z. *Russ. Chem. Rev.* **1999**, *68*, 345. (c) Kinoshita, M. *Phil. Trans. R. Soc. London, Ser. A* **1999**, *357*, 2855. (d) Miller, J. S.; Epstein, A. J. *Chem. Commun.* **1998**, *13*, 1319. (e) Miller, J. S.; Epstein, A. J. *Angew. Chem., Int. Ed. Engl.* **1994**, *33*, 385. (f) Miller, J. S. *Chem. Soc. Rev.* **2011**, *40*, 3266.

(2) Miller, J. S.; Calabrese, J. C.; Epstein, A. J.; Bigelow, R. W.; Zhang, J. H.; Reiff, W. M. *J. Chem. Soc., Chem. Commun.* **1986**, 1026.

(3) Miller, J. S.; Calabrese, J. C.; Rommelmann, H.; Chittipeddi, S. R.; Zhang, J. H.; Reiff, W. M.; Epstein, A. J. *J. Am. Chem. Soc.* **1987**, *109*, 769.

(4) Chittipeddi, S.; Cromack, K. R.; Miller, J. S.; Epstein, A. J. *Phys. Rev. Lett.* **1987**, *58*, 2695.

(5) Miller, J. S. *J. Mater. Chem.* **2010**, *20*, 1846.

(6) Chittappeddi, S.; Selover, M. A.; Epstein, A. J.; O'Hare, D. M.; Manriquez, J.; Miller, J. S. *Synth. Met.* **1989**, *27*, B417.

(7) Varret, F.; Nogues, M.; Goujon, A. In *Magnetism: Molecules to Materials*; Miller, J. S., Drillon, M., Eds.; Wiley-VCH: New York, 2000; Vol. *1*, p 257.

(8) Kobayashi, H.; Kobayashi, A.; Cassoux, P. *Chem. Soc. Rev.* **2000**, *29*, 325.

(9) Ratera, I.; Veciana, J. *Chem. Soc. Rev.* **2012**, *41*, 303.

(10) Coronado, E.; Day, P. *Chem. Rev.* **2004**, *104*, 5419.

(11) Her, J.-H.; Stephens, P. W.; Ribas-Ariño, J.; Novoa, J. J.; Shum, W. W.; Miller, J. S. *Inorg. Chem.* **2009**, *48*, 3296.

(12) Taliaferro, M. L.; Selby, T. D.; Miller, J. S. *Chem. Mater.* **2003**, *15*, 3602.

(13) Miller, J. S.; Gantzel, P. K.; Rheingold, A. L.; Taliaferro, M. L. *Inorg. Chem.* **2009**, *48*, 4201.

(14) Huang, Z. J.; Chen, F.; Ren, Y. T.; Xue, Y. Y.; Chu, C. W.; Miller, J. S. *J. Appl. Phys.* **1993**, *10*, 6563.

(15) DaSilva, J. G.; Miller, J. S. *Inorg. Chem.* **2013**, *52*, 1108.

(16) DaSilva, J. G.; Miller, J. S. *J. Chem. Soc., Dalton Trans.* **2013**, *42*, 8334.

(17) Hamlin, J. J.; Beckett, B. R.; Tomida, T.; Shilling, J. S.; Yee, G. T. *Polyhedron* **2003**, *22*, 2249.

(18) Looney, C. W.; Falk, K.; Hamlin, J. J.; Tomida, T.; Shilling, J. S.; Haase, W.; Tomkowicz, Z. *Polyhedron* **2003**, *22*, 3339.

(19) DaSilva, J. G.; McConnell, A. C.; Miller, J. S. *Inorg. Chem.* **2013**, *54*, 4629.

(20) McConnell, A. C.; Bell, J. D.; Miller, J. S. *Inorg. Chem.* **2012**, *51*, 9978.

(21) Takeda, K.; Mito, M. In *Carbon-Based Magnetism*; Makarova, T., Palacio, F., Eds.; Elsevier: New York, 2006; p 131.

(22) Mito, M.; Takawae, T.; Takeda, K.; Takagi, S.; Matsushita, Y.; Deguchi, H.; Rawson, J. M.; Palacio, F. *Polyhedron* **2001**, *20*, 1509.

(23) Mito, M.; Fujino, M.; Komorida, Y.; Deguchi, H.; Takagi, S.; Fujita, W.; Awaga, K. *J. Phys. Soc. Jpn.* **2008**, *77*, 124713.

(24) Takeda, K.; Konishi, K.; Tamura, T.; Kinoshita, M. *Phys. Rev. B* **1996**, *53*, 3374.

(25) Thompson, J. D.; Sparn, G.; Diederich, F.; Gruner, G.; Holczer, K.; Kaner, R. B.; Whetten, R. L.; Allemand, P. M.; Li, Q.; Wudl, F. *Mater. Res. Soc. Symp.* **1992**, *247*, 315.

(26) Brandon, E. J.; Rittenberg, D. K.; Arif, A. M.; Miller, J. S. *Inorg. Chem.* **1998**, *37*, 3376. Arthur, J. L.; Moore, C. E.; Rheingold, A. L.; Lapidus, S. H.; Stephens, P. W.; Miller, J. S. *Adv. Funct. Mater.* **2012**, *22*, 1802.

(27) Nakano, M.; Sorai, M. *Mol. Cryst. Liq. Cryst.* **1993**, *233*, 161.

(28) Chakraborty, A.; Epstein, A. J.; Lawless, W. N.; Miller, J. S. *Phys. Rev. B* **1989**, *40*, 11422.

(29) Lawless, W. N.; Clark, C. F.; Arenz, R. W. *Rev. Sci. Instrum.* **1982**, *53*, 1647.

(30) (a) Mydosh, J. A. In *Spin Glasses: An Experimental Introduction*; Taylor and Francis: London, 1993, p 67. (b) ϕ is a parameter indicative of the amount of spin disorder in a material: $\phi = \Delta T_{max}/[T_{max}(\Delta \log \omega)]$, where ΔT_{max} = difference between peak maximum of the temperatures at the high and low frequencies, T_{max} = peak maximum of the temperature at low frequency, $\Delta \log(\omega)$ = difference in the logarithms of the high and low frequencies (ω).
(31) Taliaferro, M. L.; Palacio, F.; Miller, J. S. *J. Mater. Chem.* **2006**, *16*, 2677.
(32) Or an almost compensated ferrimagnet, which is highly unlikely due to the differing nature of the spin-carriers involved in the system.
(33) Bhowmick, I.; Hillard, E. A.; Dechambenoit, P.; Coulon, C.; Harris, T. D.; Clérac, R. *Chem. Commun.* **2012**, *48*, 9717.
(34) The terms canted antiferromagnet and weak ferromagnet are used interchangeably [Carlin, R. L. in *Magnetochemistry*; Springer-Verlag: Berlin, 1986; pp 148−9] with small canting angles being associated with dominant antiferromagnetic behavior. Nevertheless, it seems more appropriate to associate large canting angles (approaching 180°) with dominant antiferromagnetic behavior and small canting angles (approaching 0°) with dominant ferromagnetic behavior. Using this definition, materials with canting angles >90° and <90° should be called canted antiferromagnets and weak ferromagnet, respectively. Using this convention, as discussed in the text, the canting angle is calculated from $2\arccos[2M_r(P)/M_s(P)]$ and not with an arcsin function as it is reported for example in ref 33.
(35) (a) Binder, K.; Young, A. P. *Rev. Mod. Phys.* **1986**, *58*, 801. (b) Maryško, M.; Jirák, Z.; Hejtmánek, J.; Knížek, K. *J. Appl. Phys.* **2012**, *111*, 07E110. (c) Weng, D.-F.; Wang, Z.-M.; Gao, S. *Chem. Soc. Rev.* **2011**, *40*, 3157.
(36) (a) Stryjewski, E.; Giordano, N. *Adv. Phys.* **1977**, *26*, 487. (b) Hysteresis is not an attribute of a metamagnet. However, several examples of metamagnets exhibit hysteresis, and this is ascribed to non-compensated canting leading to weak ferromagnetic (canted antiferromagnetic) behavior, e.g.: Zhang, D.; Wang, H.; Chen, Y.; Ni, Z.-H.; Tian, L.; Jiang, J. *Inorg. Chem.* **2009**, *48*, 11215. Sun, Q.; Cheng, A.; Wang, Y.-Q.; Ma, Y.; Gao, E.-Q. *Inorg. Chem.* **2011**, *50*, 8144. Colacio, E.; Ghazi, M.; Stoeckli-Evans, H.; Lloret, F.; Moreno, J.; Perez, P. *Inorg. Chem.* **2001**, *40*, 4876. Yang, C.; Wang, Q.-L.; Qi, J.; Ma, Y.; Yan, S.-P.; Yang, G.-M.; Cheng, P.; Liao, D.-Z. *Inorg. Chem.* **2011**, *50*, 4006. Keene, T.; Light, M.; Hursthouse, M.; Price, D. *Dalton Trans.* **2011**, *40*, 2983. Numata, Y.; Inoue, K.; Baranov, N.; Kurmoo, M.; Koichi, K. *J. Am. Chem. Soc.* **2007**, *129*, 9902. Weng, D.-F.; Wang, Z.-M.; Gao, S. *Chem. Soc. Rev.* **2011**, *40*, 3157. Rouco, A.; Obradors, X.; Tovar, M.; Pérez, F.; Chateigner, D.; Bordet, P. *Phys. Rev. B* **1994**, *50*, 9924. Colacio, E.; Domínguez-Vera, J. M.; Ghazi, M.; Kivekäs, R.; Lloret, F.; Moreno, J. M.; Stoeckli-Evans, H. *Chem. Commun.* **1999**, 987. Gao, E.-Q.; Wang, Z.-M.; Yan, C.-H. *Chem. Commun.* **2003**, 1748. Yuan, A.-H.; Qian, S.-Y.; Liu, W.-Y.; Zhou, H.; Song, Y. *Dalton Trans.* **2011**, *40*, 5302. Liu, D. S.; Sui, Y.; Wang, T. W.; Huang, C. C.; Chen, J. Z.; You, X. Z. *Dalton Trans.* **2012**, *41*, 5301. Huang, Z.-L.; Drillon, M.; Masiocchi, N.; Sironi, A.; Zhao, J.-T.; Rabu, R.; Panissod, P. *Chem. Mater.* **2000**, *12*, 2805. Zheng, Y.-Z.; Xue, W.; Tong, M.-L.; Chen, X.-M.; Grandjean, F.; Long, G. J. *Inorg. Chem.* **2008**, *47*, 4077. Jia, Q.-X.; Tian, H.; Zhang, J.-Y.; Gao, E.-Q. *Chem.—Eur. J.* **2011**, *17*, 1040.
(37) Shum, W. W.; Her, J.-H.; Stephens, P. W.; Lee, Y.; Miller, J. S. *Adv. Mater.* **2007**, *19*, 2910.